GOSPODARKA SUROWCAMI MINERALNYMI

Tom 24 2008 Zeszyt 4/3

T. KURAKAMI*, J. YAMATOMI**, R. SATO*, Y. SAGAWA***, S. MURAKAMI**

Mining with backfill at the Hishikari Mine, Japan

1. Mining operation at the Hishikari Mine

The Hishikari Mine, located at southern Kyushu district in Japan (Fig. 1), produced 183,000 tonnes of ore, with gold grade of 46 g/t in 2007. The Hishikari gold deposit was discovered by the Metal Mining Agency of Japan (a precursor of JOGMEC: Japan Oil, Gas and Metals National Corporation) in 1981. Subsequent exploration and development by

Fig. 1. Location map of the Hishikari Mine

Rys. 1. Lokalizacja kopalni Hishikari

* Sumitomo Metal Mining Co., Ltd., Hishikari Mine, Kagoshima, Japan.
** The University of Tokyo, Tokyo, Japan.
*** Sumitomo Metal Mining Oceania Pty. Ltd., Northparkes Mines, New South Wales, Australia.

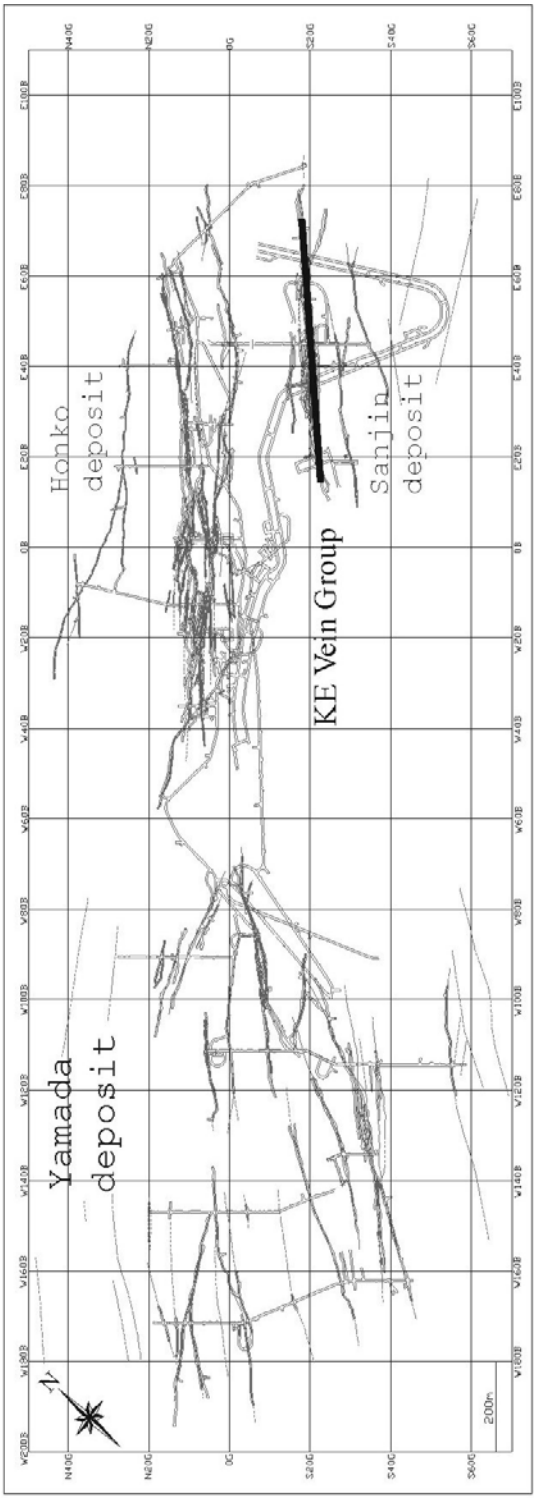

Fig. 2. Plan view of the Hishikari mine underground

Rys. 2. Widok kopalni podziemnej Hishikari

Sumitomo Metal Mining Co., Ltd. (SMM), the property owner, have proved Hishikari to be one of the outstanding gold deposits in the Japanese mining history (Ueno 1993). The Hishikari Mine consists of three deposits, namely Honzan, Yamada and Sanjin (Fig. 2). The veins are extracted mainly by drifting and bench stoping with backfill. Blasted waste rocks are generally used as backfill materials.

In the earliest years, bench stoping of smaller dimension with the height of 11 m was adopted. Then the engineering evaluation of rock mass was employed, and as the mining operators have advanced in skill and experience, the stope dimension has been getting larger (Sato, Terashima 2007). Today the height of stope dimension is 19 m in the Honzan district and 24 m in the Yamada district of the mine (Fig. 3).

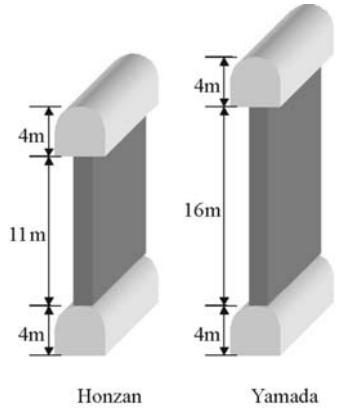

Fig. 3. Current major stope dimension at the Hishikari Mine

Rys. 3. Bieżący wymiar głównego przodku w kopalni Hishikari

Large stope dimensions in bench stoping make it possible to achieve higher productivity, but have a risk of inducing instability of the stope. Backfilling controls the displacement of excavation surface and increases the stope stability, but practical evaluation for stope dimension in conjunction with backfilling effects is not established yet. In this paper, we have proposed an approach to evaluate supporting effects of backfilling by using numerical analyses.

2. Bench stoping

2.1. Bench Stoping

Bench stoping is predominantly employed at the Hishikari Mine. The mine comprises epithermal gold veins developing almost sub-vertically, and each vein usually has a width ranging from 0.5 m to 5 m. The veins are extracted mainly by drifting with vertical spacing of 15 m to 20 m and by bench stoping with backfill. Blasted waste rocks are generally used as backfilling materials.

Q-system has been applied to the ground support design for drifting. For bench stoping, Stability Graph Method based on Q-system was introduced for evaluating stope wall quality and stope dimension, and consequently the height of stope was determined 24 m. The result indicated that unfilled span was infinite with the average rock quality of the mine, but on the safer side, unfilled span was chosen as 12 m to 13 m conservatively (Hamamoto, Sagawa 2000). In addition, the stope opening was decided to be completely backfilled to prevent any risk of collapse. As stope dimension got higher, it became harder to drill longer holes. In order to solve this problem, upward drilling of lower half of stope was employed, and lower half of stope was excavated in advance (Fig. 4). The new layout of bench stoping resulted in improvement of blasting practice because of free face with shorter burden.

2.2. Test stoping in the KE-3 vein

The Hishikari Mine consists of three deposits, namely Honzan, Yamada and Sanjin. Supporting effects of backfilling were studied at the KE-3 (Keisen-3) vein of the Sanjin deposit. The KE-3 has a 2 m to 3 m width and a very high grade of around 100 g/t.

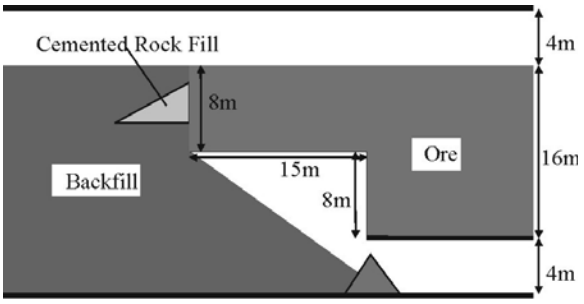

Fig. 4. Layout of Bench Stoping

Rys. 4. Rozplanowanie wyrobiska wybierkowego

Due to ventilation problems, the KE-3 vein located between –5 and 25 m sea levels was extracted by the 34 m high bench stoping. The stope height was higher than the ordinal stope height described in Figure 4. In order to increase the stope stability of the larger sized stope, the cemented crushed rock fill was tested. During this test, the stope stability of the KE-3 vein was evaluated by numerical analyses and field measurements, and the approach required for design of effective backfill support was newly developed.

3. Approach to estimate supporting effects of backfilling

The new approach that utilizes ground response curves of bench stoping and available support lines of backfilling was developed. For these purposes, we have used a three dimensional model (3D FEM) to simulate bench stoping in the KE-3 vein, repeating

excavation and backfilling, and we have obtained ground response curves and available support lines by numerical analyses.

3.1. Supporting effects of stope ends

At first, we have evaluated supporting effects of stope ends, usually consisting of competent rock and/or unmined ore that can afford to restrict wall displacements of the stope and consequently that can support the mined-out space partially. In order to assess the supporting effects of stope ends, 3D elasto-plastic analyses would be more appropriate, since in actual cases the stope ends and/or stope walls might not be completely competent but have damages to some extent. However, one elasto-plastic calculation usually requires a fair amount of time. Therefore, the supporting effects of stope ends were evaluated by combination of 2D elasto-plastic and 3D elastic analyses for practical reasons. We chose the PHASE^2, Rocscience Inc., in 2D analyses and the 3D-σ, GEOSCIENCE RESEARCH LABORATORY Co., Ltd., in 3D analyses. Both numerical packages are based on FEM.

The 3D model, shown in Figure 5, has the stope dimension of 3.0 m in width, 19.0 m in height, and 70 degrees inclination. In order to quantify the supporting effects of stope ends, we have employed a series of 3D models with different strike lengths, L, of 10 m to 140 m and calculated the horizontal convergences between wall points located at the mid-span and mid-height of the stopes. The in-situ state of stress used for the 3D FEM analyses is as follows; namely, the major principal stress, σ_1, acting parallel with the dip of stope walls is 8 MPa, the minor principal stress, σ_3, acting perpendicularly to stope walls is 2.4 MPa, and the intermediate principal stress, σ_2, acting along the strike is 8 MPa. It is assumed the models consist of homogeneous and elastic rock with Young's modulus, E_{rock}, of 17 GPa and Poisson ratio, ν, of 0.2.

We have computed the wall displacements of a series of 3D models with L = 10 m to 140 m. Internal pressure, to be equivalent to the supporting pressure provided by stope ends and acting on the walls, P_i, could be calculated by the following equation (Sagawa, Yamatomi 2003).

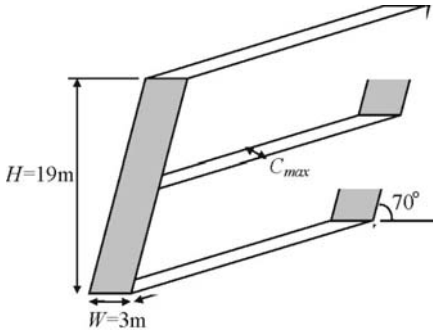

Fig. 5. Three-dimensional elastic analysis model

Rys. 5. Trójwymiarowy model analizy elastycznej

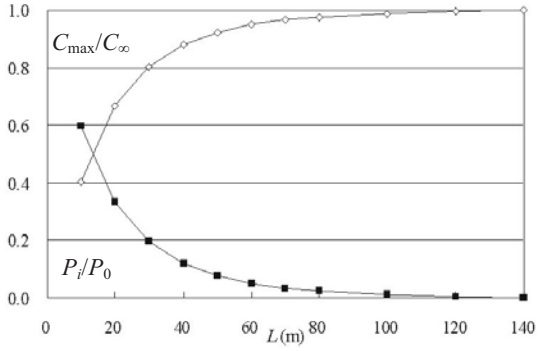

Fig. 6. The changes of maximum convergence and corresponding internal pressure produced by stope ends with different stope lengths

Rys. 6. Zmiany maksymalnej zbieżności i odpowiedniego ciśnienia wewnętrznego wytwarzanego przez krańce przodku o różnych długościach przodku

$$P_i / P_0 = 1 - C_{\max} / C_\infty \tag{1}$$

where P_0 is the stress component acting initially and vertically on the walls prior to excavation, and $C_{\max}$ is the horizontal convergence between walls at the middle of the stope in a cross-section. The C_∞ is the convergence in case of the stope with infinite strike length, i.e. $L = \infty$. Equation 1 represents the ground response curve. Changes of $C_{\max}/C_\infty$ and corresponding P_i/P_0 with different L are shown in Figure 6. The longer strike length can result in the lesser amount of supporting effects of stope ends. In Figure 6, supporting effects are 12% at L = 40 m and negligibly small at L = 140 m.

3.2. Available support lines of backfill

Backfilling controls the displacement of excavation surface and increases the stope stability. The graph plotting the support pressure available from support against wall displacement is called the support reaction line (Fig. 7). The point of most interest and practically meaningful is the point of intersection between the ground response curve and support reaction line, where equilibrium between ground and support has been achieved (Hudson et al. 2000). As can be seen from Figure 7, the location of crossing depends on when the support exhibits the ability of supporting and how high the support stiffness is. In this section, the process of how to obtain the available support lines of backfilling (start pressure of backfill support and support stiffness) is described by 3D FEM analysis using the "Excavation-Backfilling" analysis model (Fig. 8).

The "Excavation-Backfilling" analysis model repeats excavation and backfilling using the 3D model with the longest strike length of 40 m (L = 40 m). The length of each excavation is 5 m. We have analyzed behaviors of the "Excavation-Backfilling" model, changing the unfilled spans, from 5 m to 20 m. Figure 8 shows the model of unfilled span = 5 m.

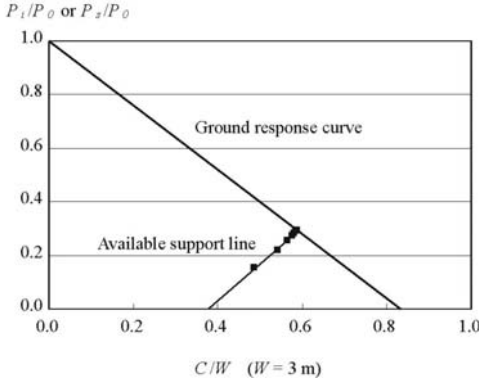

Fig. 7. Ground response curve and available support line

Rys. 7. Krzywa reakcji gruntu i dostępna linia nośna

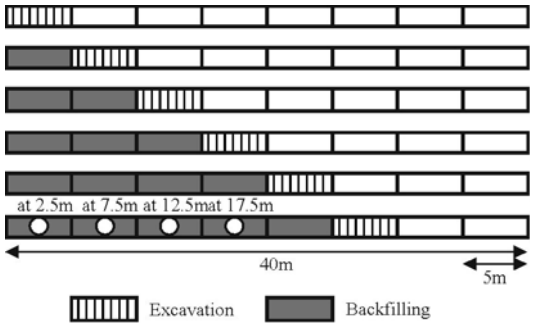

Fig. 8. Schematic illustration of the "Excavation-Backfilling" analysis model used for evaluating the support effect of backfilling

Rys. 8. Ilustracja poglądowa modelu analizy „Wyrobisko – podsadzanie" stosowanego do oceny wpływu podsadzania

As described in Section 3.1, the "Excavation-Backfilling" analysis model has supporting effects of stope ends. So, we set reference points at 2.5 m, 7.5 m, 12.5 m and 17.5 m from the left stope end of the model, as shown in Figure 8.

The computational results of horizontal convergences at the reference points were collected, and then the convergences C and C_{unfill}, when backfilled and unbackfilled, respectively, were used to calculate the support pressure of backfill, P_s, from the equation, $P_s/P_0 = 1 - C/C_{unfill}$ where P_0 is the stress component acting initially on the walls. As shown in Figure 7, the available support line of backfill is drawn from relation of C/W (W: width of stope) and P_s/P_0.

In the present study, Young's modulus of rock mass is 17 GPa, and that of backfill is 1.7 GPa. As excavation proceeds, the supporting effects of stope ends decrease and the convergences of C and C_{unfill} increase. In addition, the ground response curve changes its slope depending on unfilled span. The available support lines with different unfilled spans are shown in Figure 9.

Based on available support lines, the support characteristics of backfill are evaluated. As shown in Figure 10, the slope of the available support line defines the support stiffness, K_s. Moreover, from the starting end of the support line we can identify the start pressure of backfill support, P_s/P_0. The support characteristics of backfill, P_s/P_0 and K_s, were obtained from the analyses, and are tabulated in Table 1. When the unfilled span is getting longer, both of the start pressure and stiffness of backfill support decrease, which results in the lower support pressure and larger wall displacement at final equilibrium. The reference points have different ground response curves and available support lines, because stope ends have supporting effects. The support stiffness, K_s, is different, but the difference in the start pressure of backfill support, P_s/P_0, is insignificant. In the next chapter, we will show the 3D elastic and 2D elasto-plastic analyses applied to the bench stoping at the Hishikari Mine. The process described in this section is used to evaluate the supporting effects of backfilling.

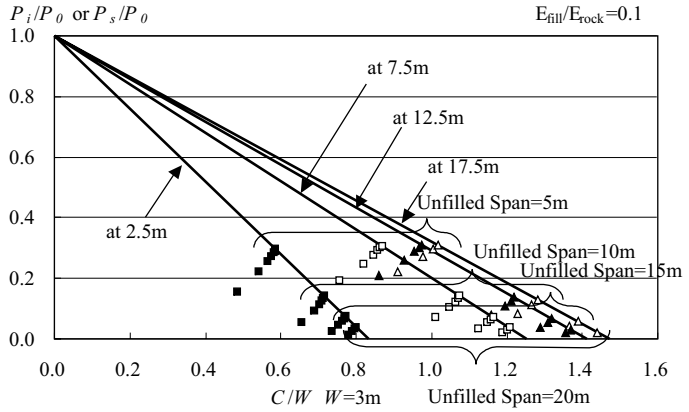

Fig. 9. Ground and support interactions with different unfilled spans at the reference points designated in Figure 8

Rys. 9. Interakcje gruntu i podpór o różnych niewypełnionych przestrzeniach w punktach referencyjnych wyznaczonych na rys. 8

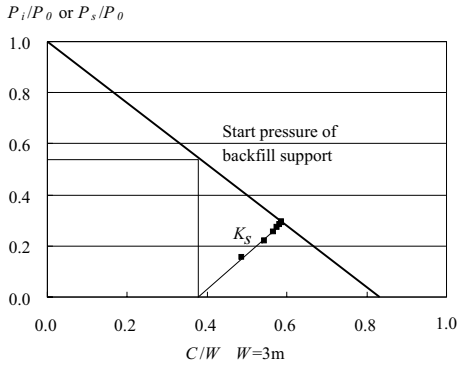

Fig. 10. The process to identify the start pressure of backfill support and calculating the support stiffness

Rys. 10. Proces identyfikacji ciśnienia początkowego podpory podsadzki i obliczanie sztywności podpory

TABLE 1

Start pressure of backfill support and the support stiffness

TABELA 1

Ciśnienie początkowe podpory podsadzki i sztywność podpory

Unifille Span [m]	P_s/P_0				K_s			
	points [m]				points [m]			
	2.5	7.5	12.5	17.5	2.5	7.5	12.5	17.5
5	0.546	0.547	0.558	0.570	1.387	1.001	0.879	0.796
10	0.255	0.245	0.239	0.233	1.416	1.047	0.930	0.826
15	0.138	0.129	0.120	0.106	1.326	0.971	0.870	0.796
20	0.076	0.070	0.060		1.208	0.846	0.787	

4. Supporting effects of backfilling at the Hishikari Mine

4.1. Uniaxial compressive test of cemented rock fill

The KE-3 vein was extracted by bench stoping with backfill. The crushed rock fill was used partially to increase the stope stability. In the case of cemented rock fill, the rock size was preferably uniform. Therefore, the Hishikari Mine used the crushed rock with the size of 20 to 50 mm generated during the color ore sorting.

The uniaxial compressive test of the cemented rock fill was conducted. The binder content was 4.5%, and the size was 12.5 cm in diameter and 25 cm in height. The uniaxial stress and strain curve of the crushed rock fill with cement was shown in Figure 11. It is noted

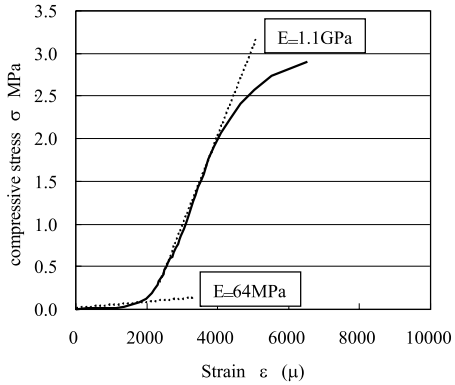

Fig. 11. The uniaxial stress and strain curve of the crushed rock fill with cement

Rys. 11. Wykres naprężenia jednoosiowego i odkształcenia wypełnienia tłuczniem z cementem

that the Young's modulus of fill specimen in early loading stage is quite as low as 50 to 100 MPa, but it increases with loading up to 0.5 to 1 GPa in the linear portion of the stress and strain curve. It is considered that the backfill actually stored in the stope is probable to show the gradual increase in stiffness with compaction caused by the surrounding wall deformation. With these facts in mind, the numerical analysis in Section 4.3 was conducted.

4.2. Field measurements of rock mass

The extensometers were installed and rock displacements were monitored to clarify supporting effects of the backfill used at the stope. We have used the extensometer, SMART MPBX (Multi-Point Borehole eXtensometer) produced by Mine Design Technologies Inc. in Canada. To observe rock displacements induced around bench stoping in the KE-3 vein, the KE-2 vein drift next to the KE-3 was used for monitoring. Six SMART MPBXs were installed horizontally and another three were installed obliquely upward from the KE-2 10 ML drift (Fig. 12).

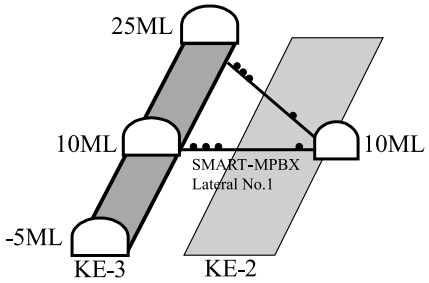

Fig. 12. Installation of SMART-MPBX extensometers

Rys. 12. Instalacja tensometrów SMART-MPBX

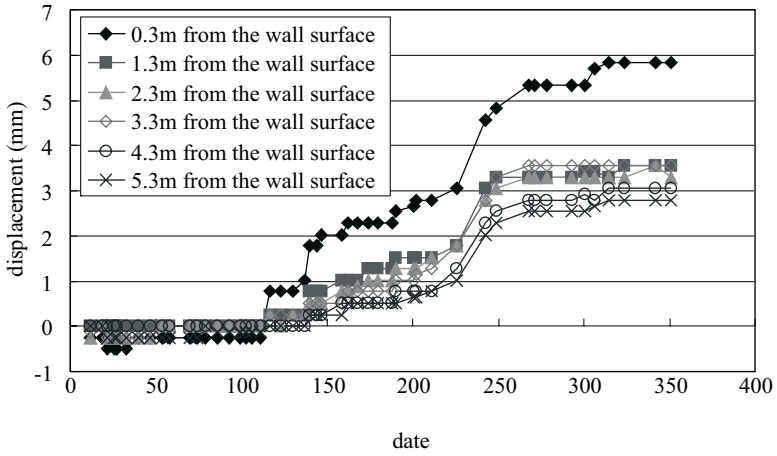

Fig. 13. Measured displacements by "SMART-MPBX Lateral No.1"

Rys. 13. Przemieszczenia mierzone przez „SMART-MPBX Lateral No.1"

The anchor located 10.3 m away from the KE-3 footwall was set as the fixed point of the extensometer, and the anchors located 0.3 m, 1.3 m, 2.3 m, 3.3 m, 4.3 m and 5.3 m away from the KE-3 footwall were set as the measurement nodes. As SMART MPBX, the displacement at the anchor points is determined by the movement of the wipers along the potentiometer. Each of instruments makes use of an electronic readout head containing six linear potentiometers and one of in-situ measurement results is shown in Figure 13.

4.3. Numerical approach

Bench stoping in the KE-3 vein was analyzed by the 3D elastic FEM model (Fig. 14) and the 2D elasto-plastic FEM model (Fig. 15). The analysis model was as same as bench stoping in the KE-3 vein located between –5 and 25 m sea levels, and the model was divided into 12 steps along the sequence of excavation-backfilling.

By 3D elastic analyses and field measurements, the initial stresses were estimated to be $\sigma_1 = 8$ MPa vertically, $\sigma_3 = 2.4$ MPa horizontally, and $\sigma_2 = 8$ MPa along the strike. Young's

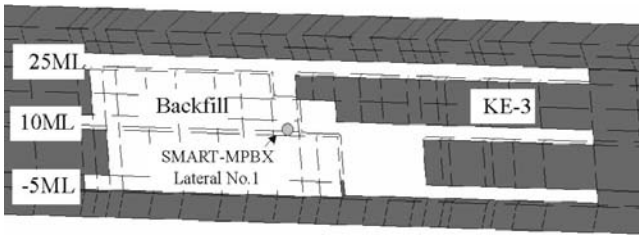

Fig. 14. 3D finite element model

Rys. 14. 3D model elementów skończonych

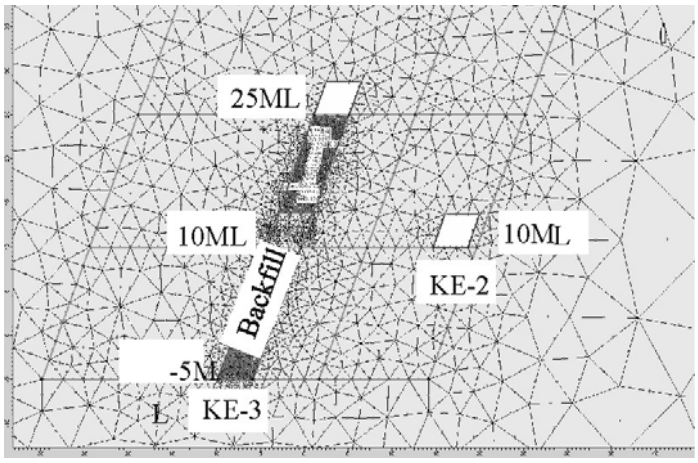

Fig. 15. 2D finite element model

Rys. 15. 2D model elementów skończonych

modulus of rock mass and backfill were assumed 5 GPa and 1 GPa, respectively, and Poisson ratios of rock mass and backfill, v, were 0.25. The supporting effects of stope ends and the support characteristics of backfill were obtained by using the process described in the former section and they are used for 2D elasto-plastic analyses.

For 2D elasto-plastic analyses, the Hoek-Brown failure criterion (Hoek et al. 2002) was used and the criterion for rock mass can be expressed as follows.

$$\sigma'_1 = \sigma'_3 + \sigma_{ci}\left(m_b \frac{\sigma'_3}{\sigma_{ci}} + s \right)^{0.5} \tag{2}$$

where σ'_1 and σ'_3 are the major and minor effective principal stresses at failure, σ_{ci} (=102.7 MPa) is the uniaxial compressive strength of intact rock material, and m_b and s are material constants defined as follows.

$$m_b = m_i \exp\left(\frac{GSI - 100}{28 - 14D} \right) \tag{3}$$

$$s = \exp\left(\frac{GSI - 100}{9 - 3D} \right) \tag{4}$$

where m_i (=8.058) is a material constant for intact rocks and D is a factor that depends on the degree of disturbance caused by blast damage and stress relaxation. Currently, D is assumed as 0 of none of damage and stress relaxation.

The Geological Strength Index (*GSI*) provides a system for estimating the reduction in rock mass strength for different geological conditions (Hoek 2001). *GSI* was assumed as 50 by in-situ logging at the stope. The material parameters, α, m_r, and s_r in the PHASE^2, required for describing the post failure behaviors were selected; they were assumed as $\alpha = m_b/8$, $m_r = m_b/2$, and $s_r = s/2$ for their starting values. The rock mass property used in PHASE^2 is shown in Table 2. Young's modulus of the backfill was selected as 1 MPa, 10 MPa, 100 MPa and 1 GPa. The pressure generated by the stope ends was applied onto the excavation surface of the analysis model. The result of 2D elasto-plastic analysis is shown in Figure 16. The result indicates that the Young's modulus of the backfill significantly influences the rock displacements.

The pressure induced from the stope ends are generally removed step by step, and rock displacements and support pressure can be calculated when the KE-3 vein have excavated completely. P_s/P_0 is found from the equation, $P_s/P_0 = 1 - C/C_{unfill}$ as described in Section 3.2. The convergences, C and C_{unfill}, when backfilled and unbackfilled, are found from the analyses results. The pressure of backfill support, P_s, is found from the equation, where P_0 is the stress component acting initially on the walls. From the analysis results in Figure 16,

relationship between Young's modulus and internal pressure, P_s/P_0, at equilibrium is shown in Figure 17. When the Young's modulus of the backfill is 1 GPa, P_s/P_0 is close to 1, and rock displacements are found rarely occurred.

From the uniaxial stress and strain curve of the cemented rock fill shown in Figure 12, the more strain develops, the more Young's modulus stiffens. As the KE-3 vein is excavated, Young's modulus of the backfill is considered to increase because it is compacted. Therefore, the available support line is used to assume the stiffening of the backfill by compaction. From the equation, $P_s/P_0 = 1 - C/C_{unfill}$, where C is the result of actual measurements, P_s/P_0 is set in each excavation step of the KE-3 vein. And from the graph of Figure 17, P_s/P_0 and corresponding Young's modulus of the backfill can be found. The numerical analyses and measurements indicate that Young's modulus of the backfill in the KE-3 vein changes from 10 MPa to 1 GPa. The rock mass deformation calculated by 2D FEM using adjustment of backfill stiffness with mining steps is fairly consistent with the measurements by the extensometer (Fig. 18). Though the supporting effects of backfill are low in early stage,

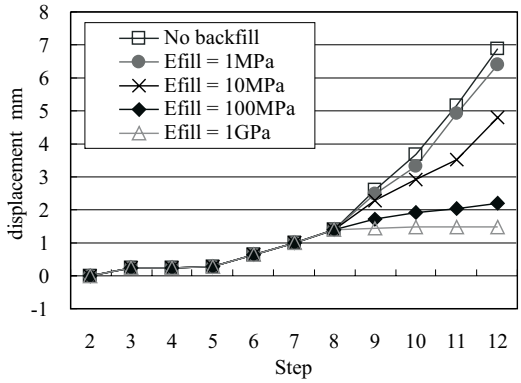

Fig. 16. Changes of rock mass deformation with different stiffness of backfill estimated by 2D FEM analyses

Rys. 16. Zmiany w odkształceniu górotworu o różnej sztywności podsadzki szacowane w analizie 2D FEM

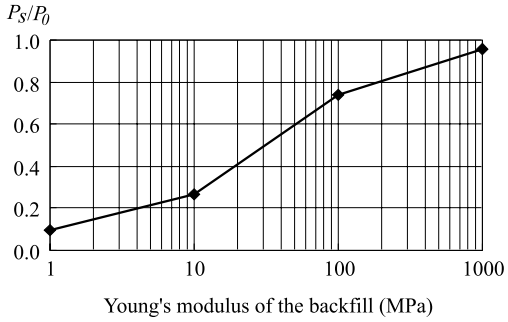

Fig. 17. Relationship between Young's modulus of backfill and internal pressure, P_s/P_0, at equilibrium obtained from Figure 16

Rys. 17. Relacja między modułem Younga podsadzki i ciśnieniem wewnętrznym, P_s/P_0, przy równowadze uzyskanej z rys. 16

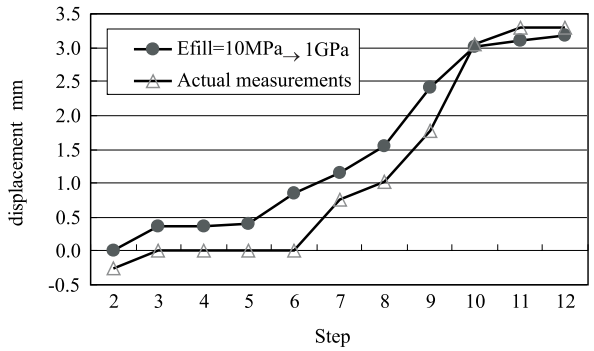

Fig. 18. Comparison of rock mass deformations measured by "SMART-MPBX Lateral No.1" and calculated by 2D FEM using adjustment of backfill stiffness with mining steps

Rys. 18. Porównanie odkształceń górotworu mierzonych przez „SMART-MPBX Lateral No.1" i obliczanych przez 2D FEM za pomocą regulacji sztywności podsadzki czynnościami eksploatacyjnymi

TABLE 2

Properties of rock mass and backfill material used in the 2D numerical analyses

TABELA 2

Właściwości górotworu i materiału podsadzki stosowanego w 2D analizach numerycznych

	GSI	E_m	v	σ_c	Peak Strength		Post-failure		
		[GPa]		[MPa]	m_b	s	α	m_r	s_r
Host Rock	50	5.0	0.25	102.7	1.351	0.004	0.169	0.676	0.002
Backfill		1.0	0.25						

GSI: Geological Structure Index.

later it can significantly develop stiffness by compaction and consequently restrict rock deformations.

Conclusions

Large stope dimensions of bench stoping have a risk of inducing instability of the stope. Backfilling increases the stope stability, but practical evaluation for stope dimension in conjunction with backfilling effects has not been established yet. So the supporting effects of backfill have been considered for bench stoping at the Hishikari Mine.

3D elasto-plastic analyses would be more appropriate, but one elasto-plastic calculation usually requires a fair amount of time. Therefore, the supporting effects of stope ends were evaluated by combination of 2D elasto-plastic and 3D elastic analyses for practical reasons. At first, the supporting effects of stope ends are identified by 3D elastic analyses, corresponding pressure is given to the excavation surface of 2D analysis model. The

supporting effects of backfill are also regarded as the support pressure given to the excavation surface.

For these purposes, we have successfully established the numerical approach to obtain the support characteristics of backfill by using "Excavation-Backfilling" model. The results indicate that the longer unfilled span makes the timing of starting pressure of backfill delayed and the stiffness of backfill support lowered. As a result, the longer unfilled span induces the larger wall displacements at final equilibrium. Thereafter, we have analyzed the supporting effects of stope ends and backfill by using the newly developed approach and a more realistic FEM model to simulate bench stoping of the KE-3 vein at the Hishikari Mine.

The uniaxial compressive test of the cemented rock fill was conducted. The backfill stiffness is considered to be fixed but to increase with loading because of compaction. Supposing that Young's modulus of the backfill in the KE-3 vein is found to change from 10 MPa to 1 GPa, rock mass deformation calculated by 2D FEM using adjustment of backfill stiffness with mining steps is consistent with that measured by the extensometer.

In this paper, we have presented our study only on mining and backfilling of the KE-3 vein. The Hishikari Mine has the wide variety of vein dimensions and characteristics. Therefore, we expect that the newly developed approach using numerical analyses in combination with the field measurements can promote and progress more reasonable design of stopes and the backfill compositions, especially, as for binder contents.

REFERENCES

[1] Hamamoto F., Sagawa Y., 2000 – MMIJ Fall Meeting Vol. A: 99–102.
[2] Hoek E., Torres C.C., Corkum B., 2002 – Hoek-Brown failure criterion – 2002 edition. NARMS-TAC 2002 (Hammah et al. eds.): 267–273.
[3] Hoek E., 2001 – Underground Mining Methods. SME, 467–474.
[4] Hudson J.A., Harrison J.P., 2000 – Engineering Rock Mechanics. Oxford: Elsevier Science.
[5] Sagawa Y., Yamatomi J., 2003 – Stope design in the Hishikari Gold Mine, Japan, by using numerical analysis. 10th ISRM Congress.
[6] Sato R., Terashima T., 2007 – Journal of MMIJ 123: 179–183.
[7] Ueno T., 1993 – Journal of MMIJ 109: 575–580.

EKSPLOATACJA GÓRNICZA Z PODSADZKĄ W KOPALNI HISHIKARI (JAPONIA)

Słowa kluczowe

Podsadzka, podziemna kopalnia złota, obliczenia numeryczne

Streszczenie

Kopalnia Hishikari, jedyna kopalnia złota w Japonii, obejmuje epitermalną żyłę złóż Au-Ag. W 2007 roku kopalnia wyprodukowała 183.000 ton rudy, o zawartości złota 46 g/t. Żyły są wydobywane głównie poprzez roboty chodnikowe i wyrobiska wybierkowe z podsadzką. Skały odpadowe po robotach strzelniczych są sto-

sowane głównie jako materiał na podsadzkę, a okruchy skał z cementem są stosowane w większych przodkach wybierkowych. Podsadzanie reguluje przemieszczenie powierzchni wyrobisk i zwiększa stabilność przodku, ale praktyczna ocena wymiaru przodku w połączeniu ze skutkami stosowania podsadzania nie jest jeszcze określona. Opracowanie przedstawia podejście do określania skutków uzupełniających podsadzania za pomocą analiz numerycznych. Wyniki ukazują nadzwyczaj dobry wpływ na stabilność przodku z większą kompakcją i usztywnieniem podsadzki.

MINING WITH BACKFILL AT THE HISHIKARI MINE, JAPAN

Key words

Backfilling, underground gold mine, numerical calculations

Abstract

The Hishikari Mine, the only gold mine in Japan, consists of epithermal vein type Au-Ag deposits. In 2007, the mine produced 183,000 tonnes of ore, with gold grade of 46 g/t. The veins are extracted mainly by drifting and bench stoping with backfill. Blasted waste rocks are generally used as backfill materials and crushed waste rocks with cement are used for larger stopes. Backfilling controls the displacement of excavation surface and increases the stope stability, but practical evaluation for stope dimension in conjunction with backfilling effects is not established yet. So the paper presents an approach to estimate supporting effects of backfilling by using numerical analyses. The results show remarkable effects on the stope stability with more compaction and stiffening of the backfill.